SCANNING KELVIN PROBE MICROSCOPY FOR INVESTIGATION OF MICROCRYSTALLINE SILICON PIN-SOLAR CELLS

A. Breymesser, V. Schlosser
Institute for Material Physics, University of Vienna, Strudlhofgasse 4, A-1090 Vienna, Austria
Phone: +43-(0)1-586 34 08-27, Fax: +43-(0)1-586 34 08-13, Email: e8727675@student.tuwien.ac.at

D. Peiró, C. Voz, J. Bertomeu, J. Andreu
Departament de Física Aplicada i Òptica, Universitat de Barcelona, Av. Diagonal 647, E-08208 Barcelona, Spain

J. Summhammer
Atom Institute of the Austrian Universities, Stadionallee 2, A-1020 Vienna, Austria

ABSTRACT: Scanning Kelvin Probe Microscopy (SKPM) was applied on cross sections of microcrystalline silicon pin diode structures deposited by hot-wire chemical vapor deposition (HWCVD) in order to determine the potential and electric field distribution within the devices. Two different deposition approaches for the compensated absorber were investigated. In the controlled doping approach the compensated absorber was deposited by mixing a low diborane content to the gas flux. In the residuals doping approach the compensation of the absorber was achieved in the chamber for doped silicon deposition utilizing residual boron from the prior p-type layer deposition step. Comparing measurements with simulations yielded information about the actual defect and dopant distribution within the diode structures.
Keywords: Micro Crystalline Si - 1: Characterisation - 2: Surface Potential – 3

1. INTRODUCTION

In the last years microcrystalline silicon (µc-Si) thin films have attracted great attention as a new photovoltaic material. With this material it is possible to combine simple and cheap low temperature deposition techniques known from amorphous silicon with the long term stability of the photovoltaic performance like in bulk crystalline silicon solar cells. One critical point in producing microcrystalline silicon solar cells is the deposition procedure with numerous tunable parameters influencing the quality and character of the produced diode structures. Extended investigation of the material, diode and solar cell characteristics is essential in order to correlate the impact of the deposition conditions on the electrical and optical quality of the devices [1, 2].

Scanning Kelvin Probe Microscopy (SKPM) is a work function measurement method based on a Scanning Force Microscope (SFM) and a modified Kelvin probe technique. Due to the excellent lateral resolution of the SFM, work function measurements with a resolution far below the micrometer level can be carried out [3].With this method it is possible to visualize the position of the Fermi level within the forbidden band gap and the influence of the deposition conditions on it [4].

µc-Si is like crystalline silicon an indirect semiconductor. For acceptable exploitation of the usable light spectrum besides light trapping considerations a sufficient absorber thickness of some microns has to be used. To overcome the relatively low diffusion lengths in µc-Si limiting the light generated currents usually pin diode structures are applied. The thin, highly doped regions at the borders generate an electric field within the thick intrinsic absorber utilized for drift field assisted collection of charge carriers. Therefore a high quality intrinsic layer has to be grown which is not a trivial problem. Besides high purity deposition conditions avoiding incorporation of defects also compensation is used in order to obtain a layer without net doping (microdoping).

In this work µc-Si structures with compensated absorbers are investigated by SKPM. Application of this characterization method on cross sectioned µc-Si diodes shall clarify the situation about the real conditions of the potential and electric field distribution within the diodes. The results provided a feedback on the deposition process for the compensated absorber.

2. EXPERIMENTAL

The µc-Si structures were deposited by hot-wire CVD (HWCVD) at the University of Barcelona. As substrate, Corning 7059 glass coated with highly conducting n-type ZnO was used. Then the pin structure was sequentially deposited with the p-doped layer next to the ZnO. The substrate temperature during deposition was between 125°C and 215°C and the hot filament temperature was around 1700°C. The gas mixture consisted of silane and hydrogen (95% dilution) and the deposition pressure was around 1×10^{-2} mbar. For obtaining doped layers diborane or phosphine was added to the gas flux. Due to the inherent n-type character of the intrinsic µc-Si material compensation was carried out. In the controlled doping approach after deposition of the p-type layer the chamber was evacuated and a dense amorphous layer was grown without doping. Afterwards the compensated i-layer was deposited by adding a very small fraction of diborane to the gas flux. It can be assumed that a constant boron concentration was incorporated by this method. In the residuals doping approach the boron residuals in the chamber from the prior deposition step were used for compensation of the absorber grown directly after p-layer deposition without evacuation. Using this approach should yield a graded boron concentration caused by the depletion of boron in the deposition chamber.

To prepare cross sections of the µc-Si structures for SKPM two diodes were glued together with the top silicon layers facing each other and the glass substrates on the outside of the sandwich. A mirror-like cross section was

achieved by grinding and polishing. No further surface treatments of chemical or thermal kind were applied in order not to alter or destroy the structures. The cross sections were investigated right after the preparation [5].

The basis of the SKPM measurements was a commercially available SFM Topometrix Explorer 2000 which was operated in the noncontact mode in ambient air. The SKPM experiment itself was a home-built addition to the SFM. It was based on a modified classical Kelvin probe experiment. In this setup the conducting tip and sample form a kind of capacitor. Applying an AC voltage between tip and sample a mechanical tip oscillation is induced. When there is no DC potential between the tip and the sample – which in fact is the sum of an externally applied voltage and the contact potential between tip and sample due to their different work functions – the oscillation vanishes. The practical approach in the setup was to measure the electrically induced tip oscillation amplitude by lock-in technique. This information was used to generate a DC voltage by means of a regulator which was added to the AC excitation so that the tip oscillation vanishes. If this condition is met, one knows that the generated DC voltage at the regulator output is equal to the contact potential but with opposite sign. Since the contact potential is a function of the Fermi level position, one can derive information about potentials, electric fields, space charge regions and charge densities. The characterization of the actual SKPM setup yielded a contact potential resolution below 5 mV. The lateral resolution was estimated to be below 100 nm. This value can be mainly explained by the relative large distance between tip and sample caused by the unsatisfactory performance of the SFM non-contact mode [6].

The influence of semiconductor surface states on SKPM measurements can be quite tremendous. Due to Fermi level pinning the bulk properties can be screened by the surface effects. Nevertheless it could be shown that at least qualitative information on the potential distribution can be derived by SKPM.

3. RESULTS

3.1. Controlled Doping Approach

In the controlled doping approach the compensated absorber was obtained by adding a low fraction of diborane to the gas mixture after evacuation and growth of a undoped amorphous layer. Fig. 1 shows a typical cross sectional AFM topography of a diode structure. It was used to distinguish the different materials constituting the solar cell. Fig. 2 shows the corresponding SKPM image sampled simultaneously with the AFM topography. Therefore the positions within the images can be correlated. The SKPM image provides contrast due to the potential distribution within the device. The differently doped layers can be distingushed by their shading.

Fig. 3 shows the surface potential and electric field distribution of some averaged lines of fig. 2. The electric field strength is obtained by spatial derivation of the potential.

As one would expect the electric field strength has its maximum at the junctions between differently doped layers. In the middle of the compensated absorber the electric field drops to low values indicating a bad compensation condition. Charge carriers generated in this region are not sufficiently collected. This could be proved

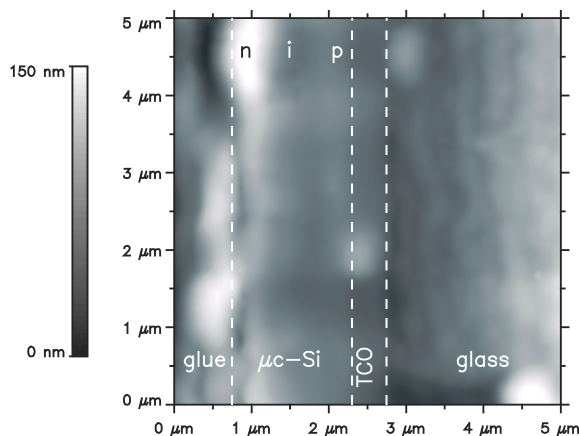

Figure 1: Cross sectional AFM topography of a μc-Si diode structure obtained by the controlled doping approach. The glass substrate is on the right and the glue on the left was used for preparational purposes.

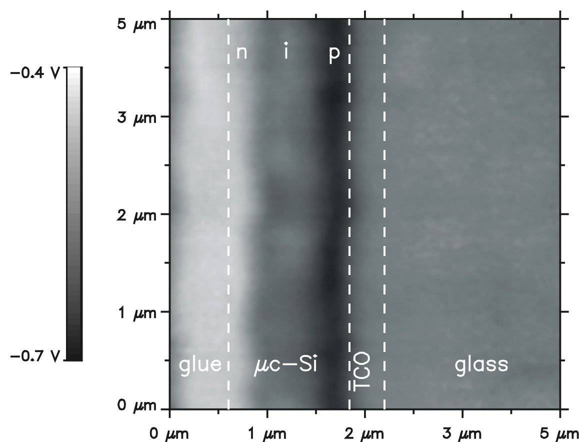

Figure 2: Cross sectional SKPM image of a μc-Si diode structure obtained by the controlled doping approach. The contrast within the μc-Si region corresponds to the potential distribution caused by dopants.

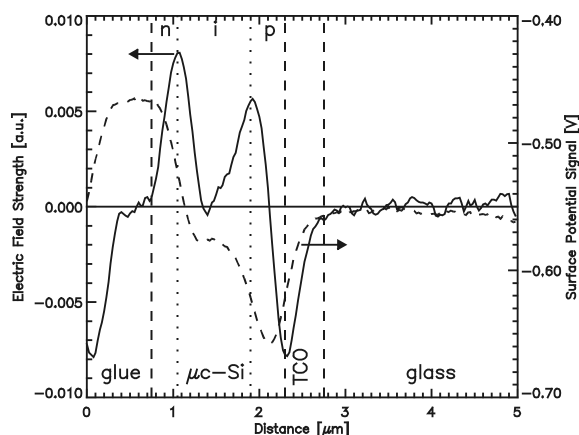

Figure 3: Surface potential signal and electric field strength of a μc-Si diode structure obtained by the controlled doping approach. The image corresponds to the averaging of some lines of fig. 2.

by spectral response measurements hinting on two charge separating regions at the n-Si/i-Si and at the i-Si/p-Si junction, respectively.

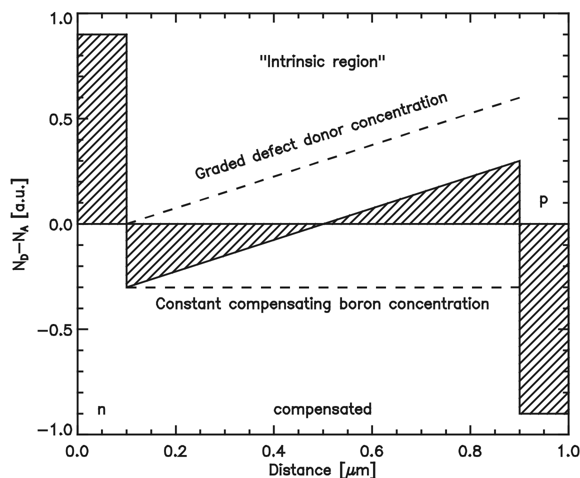

Figure 4: Suggested defect distribution for the μc-Si diode structure obtained by the controlled doping approach used for simulations.

The junction between the p-doped microcrystalline silicon and n-type TCO forms a diode with opposite polarization compared with the pin structure. The current transport at this junction happens via the amorphous tissue providing an ohmic current path. Nevertheless it has to be assumed that V_{oc} is reduced by this junction. The potential distribution within the TCO hints on the limited spatial resolution of the actual SKPM setup. The TCO should have a metal-like character due to its extensive doping. In fact, the potential changes in the layer hint on non-local tip-sample interaction limiting the spatial resolution.

Simulations using PC1D were carried out in order to clarify the situation about the actual defect distribution. From simulation results correlated to the experiments a defect distribution shown in fig. 4 was suggested. Within the compensated absorber a graded defect donor concentration and a constant compensating boron concentration is assumed. The constant boron incorporation is achieved by a constant diborane fraction in the gas flux and the graded donor concentration possibly comes from depletion of residual impurities (oxygen) in the deposition chamber. The net doping character changes in the middle of the absorber causing also a change in the majority charge carrier type.

The solar cell parameters of this device were a short circuit current density of 9.08 $mAcm^{-2}$ (absorber thickness about 900 nm), an open circuit voltage of 0.252 V, a fill factor of 43.7% and an efficiency of 1% measured under AM1.5 illumination conditions.

3.2. Residuals doping approach

In contrast to controlled the residuals doping approach was investigated as a potential candidate for improving the output of the solar cells. Two different samples deposited by the residuals doping approach were examined.

Sample A is discussed first. As can be seen in fig. 5 the surface potential and electric field distribution is completely different to the case shown in fig. 3. The potential distribution is not symmetrical within the silicon layer. At the n-Si/i-Si interface the potential has a more gentle slope than at the i-Si/p-Si interface. In the middle of the absorber the potential has only a small slope but it is different from zero. The electric field has a maximum at the n-Si/i-Si junction hinting on the change of the dopant type and a space charge region. This space charge region extends widely into the absorber which is caused by only a low dopant content. So the electric field is high in a reasonable width of the absorber. In the middle of the absorber the potential change is only gentle yielding a weak electric field. At the p-Si/TCO junction again a similar behaviour like in the sample obtained by the controlled doping approach can be found. The maximum of the electric field indicates the middle of the space charge region. Again the shape of the potential profile is not like one would expect for ideally intrinsic material. But nevertheless the situation seems to be improved due to the moderate decrease of the potential near the n-Si/i-Si junction.

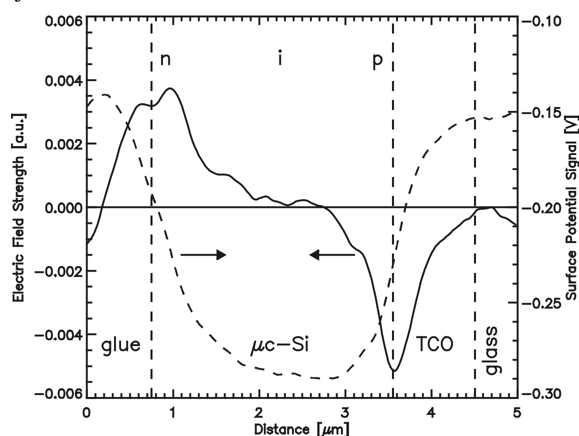

Figure 5: Surface potential signal and electric field strength of a μc-Si diode structure obtained by the residuals doping approach (sample A).

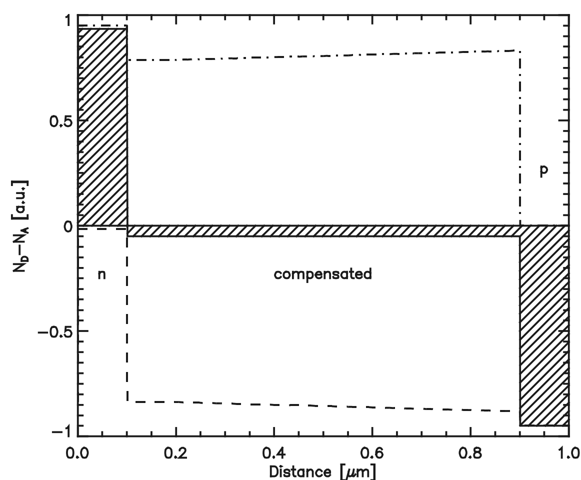

Figure 6: Suggested defect distribution for the μc-Si diode structure obtained by the residuals doping approach (sample A) used for simulations.

Again simulations were carried out in order to estimate the actual electrically active defect distribution within the device. A suggested defect distribution model can be found in fig. 6. In the compensated layer a graded donor concentration is assumed. Again this can be possibly

explained by incorporation of residual contaminants in the deposition chamber. Additionally a graded acceptor concentration is assumed where the gradation is explained by the depletion of the boron content of the chamber. In the case of the sample investigated a net p-type dopant character can be found in the compensated layer, which is equally distributed. It is remarkable that the net dopant character seems to have no gradation. The net dopant character is relatively weak.

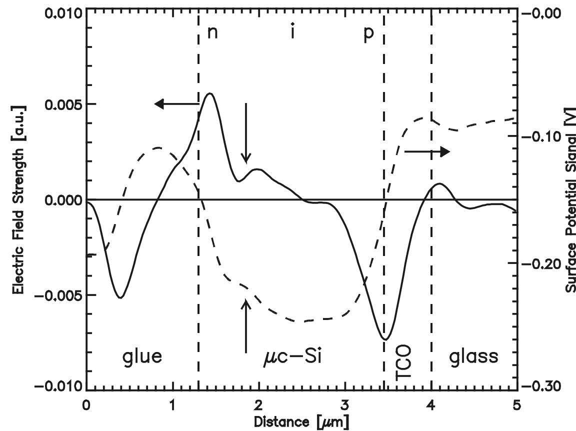

Figure 7: Surface potential signal and electric field strength of a μc-Si diode structure obtained by the residuals doping approach (sample B).

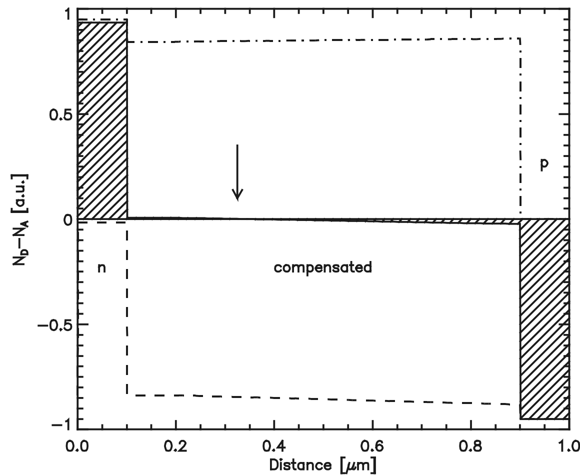

Figure 8: Suggested defect distribution for the μc-Si diode structure obtained by the residuals doping approach (sample B) used for simulations.

This was not the usual case for the samples deposited by the residuals doping approach. When the two dopant slopes in the compensated silicon layer are different a change of the dopant character can occur within the layer. This was observed with sample B. The potential and electric field distribution of sample B shown in fig. 7 is quite similar to sample A in fig. 5. The only main difference is the typical kink of the curves indicated by the vertical arrows. The origin of this kink could be clarified by carrying out PC1D simulations. The suggested defect distribution and basis for the simulations of sample B is shown in fig. 8. Again a graded defect donor concentration and a graded boron compensation is assumed. In this case the slopes of the gradations are different yielding a change of the majority charge carrier type within the absorber. Near to the p-type layer the absorber has a weak p-type character like sample A. But the situation changes at the location indicated by the vertical arrow in fig. 8: The majority charge carriers change from p-type to n-type. A consequence of this majority charge carrier change and appropriate gradation slopes is that at the location of the arrow a broad space charge region is present accompanied by a relatively high electric field. This fact should have a positive impact on the solar cell characteristics due to relatively good drift field assisted collection of charge carriers.

Sample A had a short circuit current density of 10.9 $mAcm^{-2}$, an open circuit voltage of 0.27 V, a fill factor of 37% and an efficiency of 1.1% and sample B a short circuit current density of 14 $mAcm^{-2}$, an open circuit voltage of 0.35 V, a fill factor of 51% and an efficiency of 2.5% measured under AM1.5 illumination conditions for both solar cells. Although the absorber of sample B was only 1.4 μm (sample A 1.95 μm) the short circuit current density is higher than for sample A. This is a proof for the superior charge carrier collection characteristics of sample B which is caused by the unique dopant distribution shown in fig. 8.

4. CONCLUSIONS

Although the surface restricts the measurements to qualitative statements SKPM provided access to the potential and electric field distributions within μc-Si pin diode structures on a microscopic level. Direct information on the actual dopant and defect distributions could be achieved carrying out one-dimensional PC1D simulations.

Depending on the deposition (controlled or residuals doping approach) different defect and dopant distributions were obtained having a clear impact on the solar cell characteristics. Best solar cell results were achieved for a diode structure deposited by the residuals doping approach having a graded donor defect and boron profile with a change of the majority charge carrier type in the absorber.

The microdoping approach for obtaining compensated absorbers is quite a complicated task due to the great uncertainty of the unintentionally incorporated impurities. Having direct information on the microscopic potential and electric field distribution as a feedback provides a deeper insight in processes taking place during deposition.

REFERENCES

[1] D. Peiró, J. Bertomeu, C. Voz, G. Robin, J. Andreu, Proceedings 2nd World Conference and Exhibition on Photovoltaic Solar Energy Conversion (1998) 766.

[2] C. Voz, D. Peiró, J. Bertomeu, D. Soler, M. Fonrodona, J. Andreu, Mat. Sci. Eng. B **69/70** (2000) 278.

[3] J. M. R. Weaver, D. W. Abraham, J. Vac. Sci. Technol. B **9** (1991) 1559.

[4] A. K. Henning, T. Hochwitz, J. Slinkman, J. Never, S. Hoffmann, P. Kaszuba, C. Daghlian, J. Appl. Phys. **77** (1995) 1888.

[5] A. Breymesser, V. Schlosser, J. Summhammer, phys. stat. sol. (b) **215** (1999) 855.

[6] A. Breymesser, PhD thesis (2000).